Cellular and Molecular Life Sciences (2021) 78:1729–1744
https://doi.org/10.1007/s00018-020-03608-6

ORIGINAL ARTICLE

Maternal high protein-diet programs impairment of offspring's bone mass through miR-24-1-5p mediated targeting of SMAD5 in osteoblasts

Govindraj Ellur[1,2] · Shinde Vijay Sukhdeo[3] · Md. Touseef Khan[1,2] · Kunal Sharan[1,2]

Received: 2 June 2020 / Revised: 20 July 2020 / Accepted: 22 July 2020 / Published online: 30 July 2020

Abstract

Maternal nutrition is crucial for the offspring's skeleton development and the onset of osteoporosis later in life. While maternal low protein diet has been shown to regulate bone mass negatively, the effect of a high protein diet (HP) remains unexplored. Here, we found that C57BL/6 mice fed with HP delivered offspring with decreased skeletal mineralization at birth and reduced bone mass throughout their life due to a decline in their osteoblast maturation. A small RNA sequencing study revealed that miR-24-1-5p was highly upregulated in HP group osteoblasts. Target prediction and validation studies identified SMAD-5 as a direct target of miR-24-1-5p. Furthermore, mimic and inhibitor studies showed a negative correlation between miR-24-1-5p expression and osteoblast function. Moreover, ex vivo inhibition of miR-24-1-5p reversed the reduced maturation and SMAD-5 expression in the HP group osteoblasts. Together, we show that maternal HP diminishes the bone mass of the offspring through miR-24-1-5p.

Keywords Maternal nutrition · miRNA · Smad5 · Development · Bone · High protein diet

Introduction

Evidence suggests that the origin of several diseases associated with aging occurs very early in life. Importantly, the nutritional status and environment experienced during in utero and early life developmental stages, often referred to as "programming" plays a vital role in the onset of many diseases [1–4]. Increased susceptibility of the offspring to chronic diseases, including obesity and diabetes in later life, has been linked to suboptimal in utero nutrition in both humans and animal models [5, 6]. The mechanism through which the prenatal nutrition affects the development of the age-related disease is still understudied. Epigenetic changes during in utero development, which regulates the heritable alterations in gene expression without changes in the DNA sequences, is one of the potential areas to understand the programming of diseases [7]. Mainly, changes in the expression of microRNAs (miRNA), which are short endogenous RNA molecules involved in the post-transcriptional repression of genes, contributes to the development of various pathologies [8]. However, only a few studies are depicting the role of miRNA in fetal programming.

Osteoporosis is a disorder characterized by reduced bone mass and increased incidence of fractures, which occurs in the elderly population. Reports suggest that bone development and homeostasis are also programmed [9]. Particularly, maternal nutrition seems to be vital in defining the skeletal size and the age for the onset of osteoporosis [10]. Human studies with Vitamin D have demonstrated that maternal levels of 25(OH)D during pregnancy positively correlates with the bone mineral density (BMD) of female offspring at their 9 and 20 years of age [11, 12]. Another mother–child cohort study done in Pune, India, showed that the offspring of mothers taking higher calcium-rich food had improved bone mineral content (BMC) and BMD [13]. Besides,

Electronic supplementary material The online version of this article (https://doi.org/10.1007/s00018-020-03608-6) contains supplementary material, which is available to authorized users.

✉ Kunal Sharan
kunalsharan@cftri.res.in; sharan.kunal@gmail.com

[1] Department of Molecular Nutrition, CSIR-Central Food Technological Research Institute, Mysore, India

[2] Academy of Scientific and Innovative Research (AcSIR), Ghaziabad 201002, India

[3] Department of Biochemistry, CSIR-Central Food Technological Research Institute, Mysore, India

evidence from animal models has also revealed that maternal nutrition affects the occurrence of osteoporosis in later life. In mice, Vitamin D supplementation during pregnancy and lactation has been shown to improve the offspring's bone microarchitecture at adult age [14]. Pre-suckling supplementation of calcium to the lactating rats resulted in increased bone length and BMD in the offspring even at 27 weeks of their age [15]. Protein calorie restriction during gestation not only results in under ossified fetuses [16], but the offspring can also have permanent low bone mass [17]. Similarly, excess of protein during pregnancy has also been shown to have catastrophic effects on offspring health [18].

Even when protein seems to have an important effect on fetal development and the health of the offspring, there is a big disparity in the guidelines of different countries for its daily intake targets during pregnancy. For instance, while Japan recommends less than 20% calorie from protein, Australia endorses 15–25%, whereas the United Kingdom, Europe, United States and Canada recommend 10–35% calories from protein [19]. The range of 10 to 35% calories recommendation from protein is huge as 10% protein in the diet is regarded as low and 35% protein is regarded as high. A lot of work has been done to check the effect of low protein high carbohydrate diet on the outcome of the pregnancy. Comparatively less studies are done with the maternal excess protein and low carbohydrate supplementation but data shows that the offspring of high protein fed mothers have a lower fetal growth, higher neonatal deaths, and decreased birth weights [20–22]. In terms of bone health, not much work is done on the influence of maternal high protein low carbohydrate diet (HP) on the programming of offspring's bone mass. Moreover, there is a lack of understanding regarding the cellular and, more importantly, the molecular mechanisms, whereby maternal nutrition modulates skeletal development in the offspring.

Therefore, in this study, we investigated the effect of maternal HP in the programming of offspring's bone health using C57BL/6 mice. We also evaluated the molecular basis for the cellular and micro-architectural alterations in the skeleton of the offspring caused by the maternal diet.

Materials and methods

Animals and diets

Eight to 10-week-old female C57BL/6 mice were recruited for the experiment with the prior approval of the Institutional Animal Ethical Committee (IAEC). Subsequently, they were first acclimatized to AIN-93G diet for a week, later these mice were plugged and divided into two groups. The groups were fed isocaloric control AIN-93G diet (21% calories from protein) or HP diet (36% calories from protein) throughout their pregnancy and lactation (Suppl. Table 1). All offspring were weaned on control AIN-93G diet and raised over it till their sacrifice. All Animals were housed in a 12-h light and 12-h dark cycle, with controlled temperature (22–25 °C), and humidity (50–55%).

Intraperitoneal (IP) calcein injections (20 mg/kg body weight) were administered to the animals at 6 and 3 days before the sacrifice. At sacrifice, various tissue, along with long bones and vertebra, were collected and stored appropriately until further analysis.

Skeletal staining and analysis

Alizarin red/Alcian blue staining of the newborn mice was done following the method published previously [23]. Briefly, after skin maceration in PBS solution, pups were skinned. Skinned specimens were immediately fixed with 100% ethanol overnight, followed by transfer to an acid solution containing 0.2% Alcian blue for 48 h and then dehydration in 96% ethanol. The maceration of soft tissues was performed by placing them in the basic staining solution containing 0.2% KOH and 0.5% alizarin red. Cleaning and hardening were performed by placing the skeleton in the destaining solution. Conservation of double-stained pups was performed in a 1:1 ratio of 20% each ethanol and glycerol. The photographs were taken with a scale. The ImageJ software was used for estimating fold change in the bone length of each dissected limb.

Micro-computed tomographic analysis

Micro-CT (both 2-D and 3D) analysis of excised bones was carried out using the Sky Scan 1076 µCT scanner (Aartselaar, Belgium) as described previously [24, 25].

Briefly, scanning of bone samples was performed at 9 µm resolution followed by reconstruction using Sky Scan recon software. To analyze trabecular bone, a region of interest (ROI) was drawn at 150 slices in the area of secondary spongiosa by excluding all primary spongiosa and cortical bone. For cortical bone, the trabecular region was excluded, and 100 consecutive image slides were selected for analysis using CTAn software. Quantification was done applying Batman software. Cortical and trabecular BMD of the femur was determined for the cortical and trabecular region using hydroxyapatite phantom rods of 4 mm in diameter with known BMD as reference.

Bone histology and histomorphometry analysis

Briefly, fixed vertebral samples were embedded in methyl methacrylate, and sections of 5 and 7 microns were collected using Leica microtome [26, 27].

Bone volume/tissue volume (BV/TV) was determined after staining with von kossa on 7-micron sections. Determination of the bone formation rate (BFR/BS) and mineral apposition rate (MAR) was done on unstained sections using fluorescence microscopy. Osteoblast number per bone surface (N.Ob/BS) and osteocyte number per bone area (Os.N/T.Ar) were measured following toluidine blue staining. Osteoclast cell count per bone surface (N.Oc/BS) was analyzed after TRAP staining of the sections. All these procedures were performed on undecalcified sections of the lumbar 4 vertebrae. Histomorphometric analyses were done using the Osteomeasure Analysis System (Osteometrics, Atlanta, GA, USA) [28].

Bone turn over markers analysis

Serum procollagen type 1N-terminal propeptide (P1NP) and urinary C-terminal type I collagen crosslinks (CTX-I) were assessed using an ELISA kit from the 12 W offspring of C and HP group as per the manufacturer's instructions (Elabscience).

Ex vivo primary culture of mouse calvarial osteoblasts (MCOBs)

For each experiment, about 4–6 calvaria were harvested at room temperature from newborn pups of C and HP group animals, and culture was done following the previously published method [25, 29]. Briefly, individual calvariae were isolated surgically, sutures, and the adherent tissues were cleaned by gentle scraping. Pooled calvariae were kept for repeated digestion with 0.1% dispase and 0.1% collagenase to release cells. The first digestion was discarded and the cells from the next consecutive 4 digestions were pooled and cultured in 10% fetal bovine serum (FBS) supplemented α-modified essential medium (α-MEM). Containing 1% penicillin/streptomycin, 1% non-essential amino acids (NEA) and 1 mM sodium pyruvate (complete growth medium). Cultures of MCOB were allowed to reach ~ 80% confluence for the experiments described below.

Quantitative RT-PCR analysis

Total RNA was isolated from either long bones or MCOBs of C and HP group with Trizol reagent (Invitrogen) according to the previously described methods [24, 30]. An equal amount of RNA from each sample (500 ng) was used to synthesize cDNA using reverse transcriptase cDNA synthesis kit (Applied Biosystems). SYBR Green chemistry was used to perform quantitative determination of relative expression of transcripts for all genes using specific primers. *ß actin* was used as an internal control (Suppl Table 2).

Western blotting

Protein was extracted from either long bones or MCOBs of C and HP groups using cell extraction buffer with protease and phosphatase inhibitors. Protein concentration was measured by BCA reagent (Thermo Scientific). The samples were denatured at 95 °C for 5 min in sample buffer, 30 µg of the protein was loaded and separated on 10% SDS-polyacrylamide gels and western blotting was performed according to a previously published protocol [27, 30]. Chemiluminescent detection was carried out with Sigma reagent using a Biorad Chemidoc instrument.

Bromodeoxyuridine incorporation (BrdU) proliferation assay

MCOBs from C and HP group animals were used for cell proliferation assays using the previously described method [25]. Briefly, at 70–80% confluence cells were trypsinized, and 6000 cells/well were seeded in 96 well plates in α-MEM supplemented with 10% FBS medium. Cells were allowed to adhere for 12 h then left for another 24 h. Four hours before the end of 24 h stimulation period, the cells were pulsed with BrdU labeling reagent, and BrdU incorporation was measured using a proliferation ELISA kit (Roche).

Alkaline phosphatase (ALP) assay

Briefly, 5000 cells/well were seeded in 96 well plates. Cells were cultured for 72 h in osteogenic differentiation medium containing α-MEM supplemented with 10% FBS, 10 mM β-glycerophosphate, 50 mg/mL of ascorbic acid, and 1% penicillin/streptomycin, 1% NEA and 1 mM sodium pyruvate. At the end of the incubation period, total ALP activity was measured at 405 nm using *p*-nitrophenyl phosphate (PNPP) as a substrate [31].

Mineralization assay

MCOBs were seeded in 12 well plates (50,000 cells/well) in osteogenic differentiation medium and cultured for 21 days with a change of medium every 48 h. At the end of the experiment, they were fixed and then stained with Alizarin red stain. For quantification, the stain was extracted with 10% cetyl pyridinium chloride, and absorbance was read at 570 nm [29, 32].

Ex vivo osteoclast culture

Primary osteoclasts were generated as per previously described protocols [28, 33]. Briefly, bone marrow cells (BMC) were isolated from the whole marrow of 12-week-old offspring of C and HP group and cultured overnight in

α -MEM supplemented with 10% FBS and 10 ng/mL macrophage colony-stimulating factor (M-CSF). The next day, the nonadherent cells were collected. After centrifugation, cells were cultured on a 24 well plate for 7 days in α-MEM plus 10% FBS containing 30 ng/mL M-CSF and 50 ng/mL RANKL (receptor activator of nuclear kB ligand) as differentiation inducers. In the end, the cells were fixed, and TRAP staining was performed. TRAP-positive multinucleated cells (three or more nuclei) were scored under a light microscope and presented as fold change as compared to control.

Small RNA sequencing and differential gene expression (DGE) analysis

Ex vivo cultured MCOBs from C and HP group animals were harvested and stored in RNA later (Qiagen). Then, at Genotypic Technology Pvt. Ltd, the samples were processed for RNA extraction. Small RNAs were converted to illumine sequencing libraries using the Illumina NextSeq 500 Single-end sequencing platform technologies. From the obtained libraries, DGE analysis of miRNAs was performed between the C and HP groups. Heatmaps were generated for the differentially expressed miRNAs (up/downregulated).

In silico miRNA target site prediction

In silico putative targets were screened using the following databases for the miR-24-1-5p. TargetScan (http://www.targetscan.org), miRBase (http://www.mirbase.org), miRanda (http://www.microrna.org), and miRWalk (http://zmf.umm.uni-heidelberg.de/apps/zmf/mirwalk2). These computational programs predict miRNA targets by checking the potential base pairing of the 3′ UTR of a target mRNA with the seed sequence of the miRNA.

TaqMan-based qRT-PCR assay

Whole RNA was isolated from MCOBs of C and HP group using triazole reagent, and cDNA was constructed using the TaqMan reverse transcription kit and miR-24-1-5p TaqMan miRNA assay kit (Applied Biosystems). cDNA samples were used as a template for real-time PCR (Quant Studio5, Applied Biosystems) using a master mix containing TaqMan 2× Universal PCR Master Mix and 20x TaqMan MicroRNA Assay Mix (Applied Biosystems). The mean C_t values of each sample were determined from triplicate reactions. The relative expression level of miRNA examined after normalizing the values with internal control snoRNA142.

Transfection assay and its analysis in MCOBs

Mimic of endogenous miR-24-1-5p and miRNA negative control with an inhibitor of miR-24-1-5p (AMBION) were transfected into mice osteoblast cells at 50–60% confluence at 50 nM concentration with Lipofectamine TM 3000 (Invitrogen), with reduced serum and antibiotic-free Opti-MEM according to the manufacture's instruction. BrdU proliferation, alp activity, mineralization, western blot, and qPCR were performed with the transfected cells [34, 35].

Smad5 3′ UTR cloning

The mouse *Smad5* 3′ UTR containing the miR-24-1-5p binding sequence (Gene ID: 181063) was amplified by PCR from the bone cDNA of the mouse. The PCR product was then subcloned into the pmirGLO Dual-Luciferase miRNA target expression vector (Promega). Binding-region mutations were achieved by parental plasmid PCR amplification, followed by DpnI enzyme treatment and insertion of mutated region site from Phusion ligase through site-directed mutation (Suppl Table 3 for the sequence of primers).

Luciferase reporter assay

MCOBs were grown up to ~80% confluence in α-MEM supplemented with 10% FBS. Cells were then transfected with 200 ng of the vector in which wild type or mutant form of 3′UTR of *Smad5* were cloned for 6 h in reduced serum and antibiotics-free Opti-MEM with Lipofectamine TM 3000 (Invitrogen). Cells were co-transfected with miR-24-1-5p mimic or negative control (miR control) at concentrations of 50 nM. Firefly and Renilla luciferase were measured in cell lysates using a Dual-Luciferase Reporter Assay System (Promega) on a luminometer (Spark 10M, Tecan). Renilla luciferase signal was used for normalization and as an internal control for transfection efficiency [34, 35].

Statistical analysis

All data are presented as mean ± SE. Animal experiments were performed with $n \geq 6$ mice per group. All cell culture experiments were performed at least three times. Student's t test between two groups and one-way ANOVA followed by Newman–Keuls post hoc test for more than two groups were conducted. P values ≤ 0.05 were considered as statistically significant.

Results

Effect of HP on maternal weight gain and newborn offspring's skeleton

Female C57BL/6 mice were plugged and fed with HP or control diet (C) throughout the gestation until the birth of their pups. There was no significant difference in the consumption of diet between C and HP dams (data not shown). However, HP dams gained significantly less weight as compared to C (Fig. 1a). Furthermore, the HP dams had a smaller litter size as compared to C (Fig. 1b).

At the birth of the pups, their body weight and body length were measured. We found a significant reduction in the body weight (Fig. 1c) and length (Fig. 1d) of the newborn pups in the HP group as compared to the C group.

Analysis of the changes in the skeletal mineralization patterns of the newborn pups from C and HP dams were done after alcian blue (stains cartilage) and alizarin red (stains calcified bone) staining. As shown in Fig. 1e, there was a decrease in the size of the skeleton in HP offspring along with a weaker alizarin red staining when compared to C offspring. To characterize skeletal defects in more detail, we dissected out and examined the intramembranous (skull) and endochondral ossification (sternum, scapula, humerus, femur, and tibia) centers of both the groups. HP offspring heads were reduced in size with striking differences in craniofacial regions as compared to C (Fig. 1f–h). A dorsal view of the skull, as shown in Fig. 1f, demonstrated that alizarin red was stained more weakly in the head plates with open switcher junctions at regions like parietal (pb), frontier (fb), nasal (nb) bones in HP offspring as compared to C group. Consistently, zygomatic bone (zb) (which is commonly known as cheekbone) size in HP offspring was also shorter in length as compared to C. Furthermore, a ventral view of the skull (Fig. 1g), revealed that basioccipital (bo), pterygoid (ptg), palatal process palatine (ppp) (indicated with stars), premaxilla (pmx) and tympanic ring, which supports the eardrum (indicated with arrows) regions were also weakly stained and shorter in length. The dorsoventral view of the skull (Fig. 1h), revealed a shortened exoccipital bone (eo) and mandible (md) in HP group pups when compared with C group. We next sought the differences in the endochondral ossification, where we found an aberration in the formation of both the axial and appendicular skeleton. Of note, the sternum ribcage of HP group pups was smaller in size with a concomitant decrease in ossification when compared to C group pups (Fig. 1i). Consistently, HP group pups had a significantly reduced long bones length, including scapula, humerus, femur, and tibia (Fig. 1j–r), indicating a limb outgrowth defect when compared to C group pups.

Effect of maternal HPD on the bone microarchitecture of the offspring at later ages

Next, we evaluated whether the decrease in mineralization of the skeleton in the newborns also results in a compromised bone microarchitecture at later ages. For that, the dams were given C or HP diet throughout their pregnancy and lactation, and then the pups were weaned on a control diet (Fig. 2a). The offspring were sacrificed at different stages of life, i.e., young (6 weeks), adult (12 weeks) and late adult (24 weeks) age, their body weight and length were measured. Their bones were subjected to micro-CT. Although there was no significant change in consumption of food between the groups after weaning (data not shown), a decrease in body weight and body length was found in both female and male offspring of the HP group as compared to C at all the age groups. 3D μ-CT analysis of the femur revealed a significant decrease in bone microarchitecture in HP group offspring, both females and males, at all the age groups when compared to C group (Fig. 2b). Trabecular bone mass parameters, bone volume to tissue volume ratio (BV/TV), and BMD were found significantly decreased in the HP group animals (Fig. 2c–h). While trabecular thickness (Tb.Th), trabecular number (Tb.N) and connection density (Conn.Dn), which are directly proportional to bone quality decreased, trabecular separation (Tb.Sp), trabecular pattern factor (Tb.Pf) and structure model index (SMI) that are inversely proportional to the quality of the bone were increased (Suppl Table 4). Similarly, μ-CT analysis of the offspring's femur cortical bone revealed a decrease in BMD, cortical thickness (Cs.Th) and mean moment of inertia (MMI), a bone strength indicator) along with an increase in cortical porosity (Po) in HP group animals of all the age groups and gender (Suppl Table 5).

Consistently, in tibia also a decrease in gross trabecular microarchitecture (Fig. 2i), BV/TV, BMD (Fig. 2j–o), Tb.Th, Tb.N, Conn.Dn and an increase in Tb.Sp, Tb.Pf and SMI (Suppl Table 4) were observed in both male and female HP group offspring at all the age groups when compared to C group offspring. Similarly, cortical bone parameters BMD, Cs.Th, Po, and MMI were negatively influenced in HP group animals of all the age groups (Suppl Table 5).

Effect of maternal HPD on the vertebral histology and bone remodeling in the offspring

The histological analysis was performed on the lumbar 4 vertebrae from C and HP female offspring. Vonkossa staining of the sections (Fig. 3a) showed a significant decrease in the BV/TV ratio of HP vertebra compared to C at all the age groups. The study of mineral apposition rate (MAR) and bone formation rate to bone surface ratio (BFR/BS) showed a significant decrease in HP group animal's vertebra,

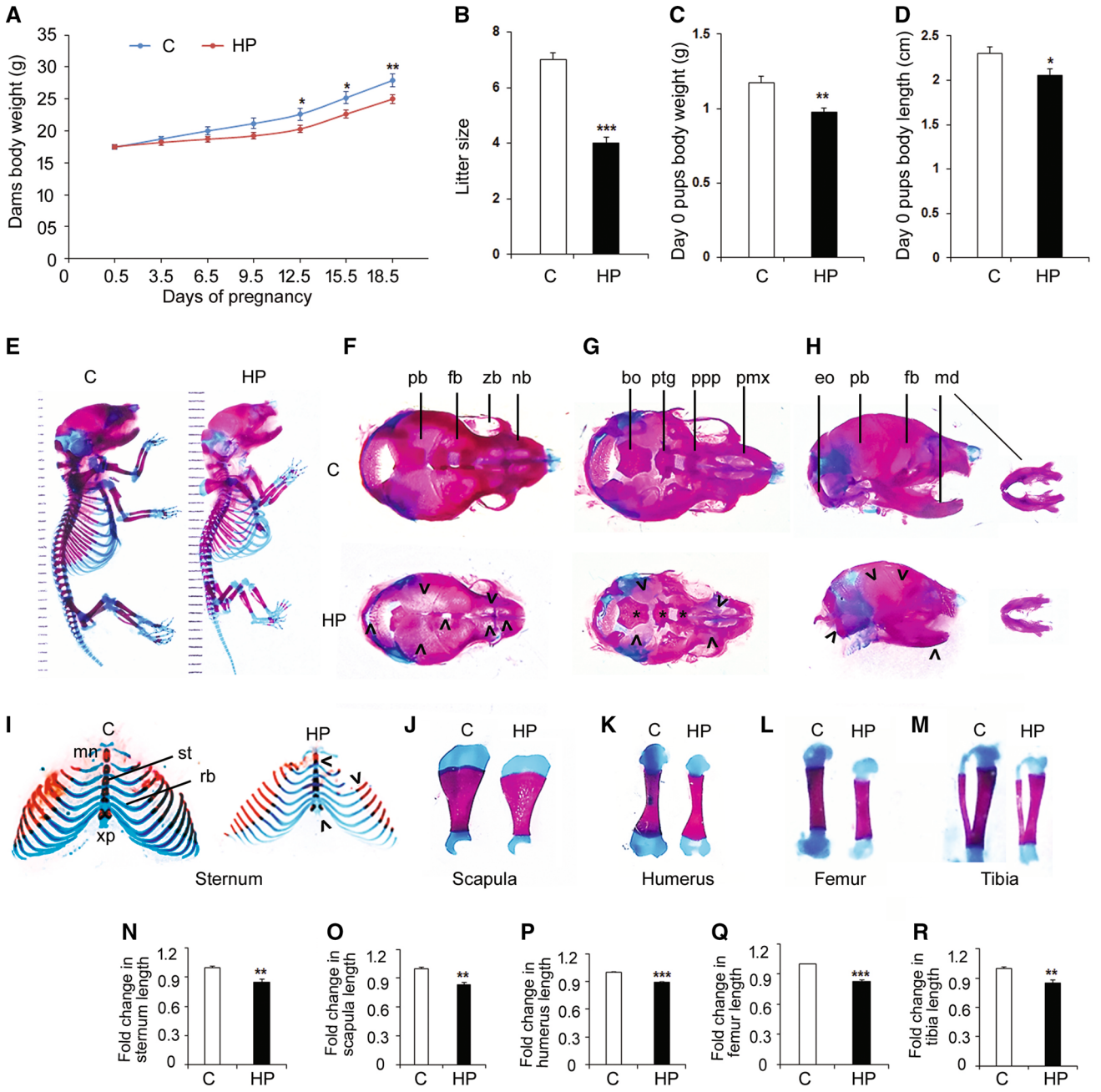

Fig. 1 Maternal HP negatively regulates the skeletal growth of the newborn offspring. **a** Effect of C and HP feeding on the body weight of the dams during gestation and **b** their litter size. **c** Effect of maternal diet on newborn offspring's body weight and **d** body length. **e** Whole-mount alizarin red and alcian blue-stained skeletons of C and HP group newborn offspring. Intramembranous ossification pattern of skull: **f** Dorsal view; **g** Ventral view; and **h** Dorsoventral view. Endochondral ossification pattern: **i** Sternum; **j** Scapula; **k** Humerus; **l** femur; and **m** Tibia. Fold change in **n** sternum length, **o** scapula length, **p** humerus length, **q** femur length, and **r** tibia length over C. Each group contains ≥ 6 animals. Data are presented as mean ± S.E.M. (*$P < 0.05$, **$P < 0.01$, ***$P < 0.001$). (*Pb* parietal bone, *fb* frontier bone, *nb* nasal bone, *zb* zygomatic bone, *bo* basiooccipital, *ptg* pterygoid, *ppp* palatal process palatine, *pmx* premaxilla, *eo* exoccipital bone, *md* mandible)

indicating a defective matrix deposition (Fig. 3b). Next, to identify the type of bone cells responsible for this effect, we first analyzed changes in the osteoblast numbers and function, which revealed a significant decline in the number of osteoblasts per bone surface (N.Ob/BS) and the number of osteocytes per tissue area (N.Os/T.Ar) in HP group. Furthermore, the analysis of osteoclast parameters showed an increase in the number of osteoclasts per bone surface (N.Oc/BS) and osteoclast surface per bone surface (Oc.S/BS) (Fig. 3b).

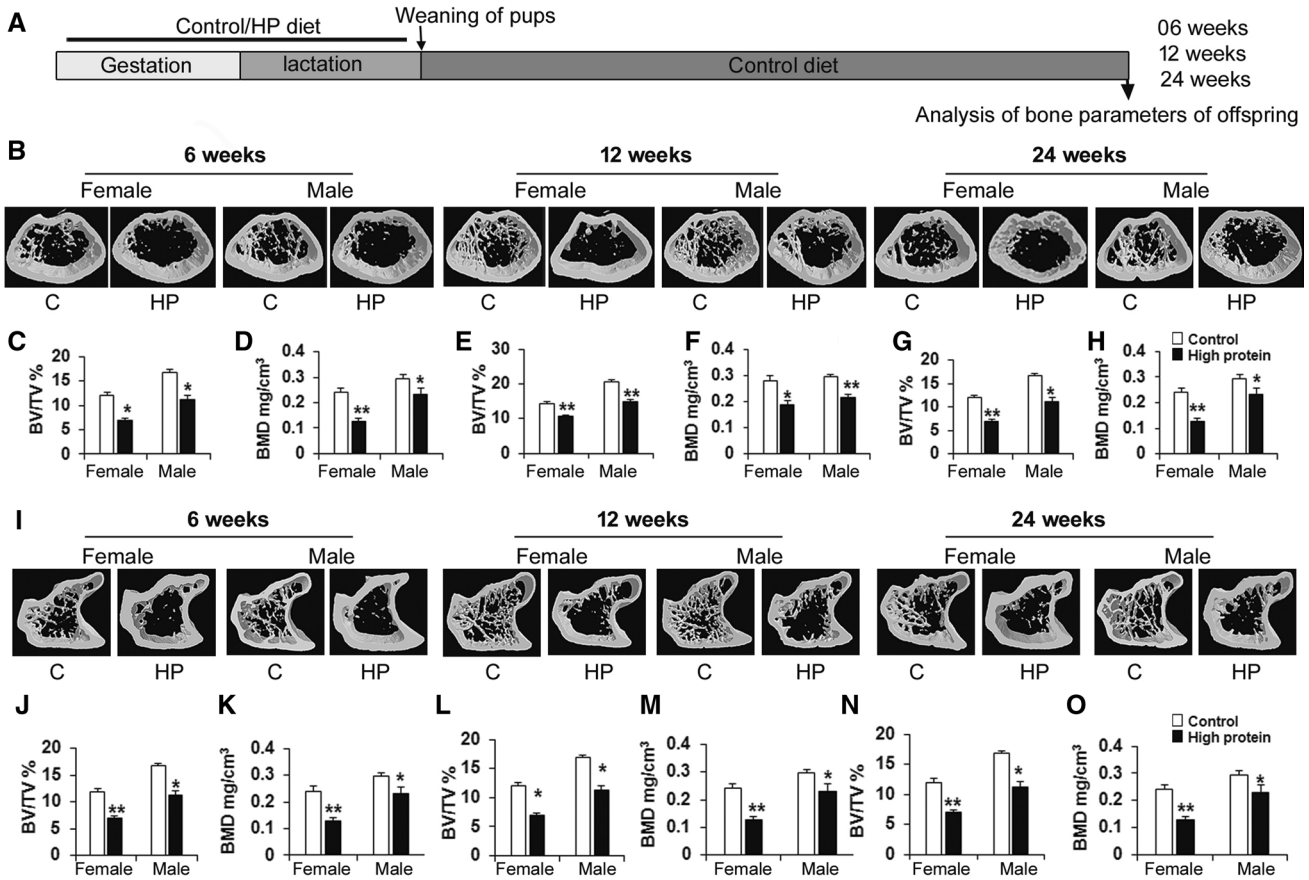

Fig. 2 Maternal HP negatively regulates the bone microarchitecture of the offspring. **a** Schematic representation of the experimental plan. **b** Representative reconstructed 3D μ-CT images of distal femur at indicated ages; **c**, **d** BV/TV (%) and BMD (mg/cm^3) of 6-week-old offspring; **e**, **f** BV/TV (%) and BMD (mg/cm^3) of 12-week-old offspring, **g**, **h** BV/TV (%) and BMD (mg/cm^3) of 24-week-old offspring. **i** Representative reconstructed 3D μ-CT images of proximal tibia at indicated ages, **j**, **k** BV/TV (%) and BMD (mg/cm^3) of 6-week-old offspring; **l**, **m** BV/TV (%) and BMD (mg/cm^3) of 12-week-old offspring, **n**, **o** BV/TV (%) and BMD (mg/cm^3) of 24-week-old offspring. Each group contains ≥ 6 animals. Data are presented as mean ± S.E.M. (*$P < 0.05$, **$P < 0.01$, ***$P < 0.001$)

Next, to determine if this negative regulation of the bone were associated with changes in the expression of genes regulating its function, we performed a qPCR analysis of key bone markers from the long bones of C and HP group's 12-week-old female offspring. The mRNA expression levels of osteoblast early differentiation marker *Runx2* (a master regulator for osteoblast differentiation), *Alp,* and late differentiation markers *Ocn, Atf4* were decreased significantly (Fig. 3c). Similar to the RNA expression, the protein expression levels of *Runx2* and *Atf4* from the long bones of HP group's adult offspring were significantly reduced (Fig. 3d, e). Moreover, *Opg* to *Rankl* ratio that is expressed by osteoblasts and is critical for osteoclastogenesis (Fig. 3f), and the expression levels of *Trap* and *CtsK*, the osteoclast differentiation markers were significantly increased in the HP group offspring bones (Fig. 3g). Consistently, the serum levels of the procollagen type 1 propeptide (P1NP), a marker for bone formation, were significantly lower (Fig. 3h) and the urinary levels of c-terminal telopeptides of collagen type 1 (CTX), a bone resorption marker was higher (Fig. 3i) in the HP group 12-week-old offspring.

Effect of maternal HPD on offspring's osteoblast and osteoclast cell function

As there were a decreased osteoblast and increased osteoclast activity in the bone sections of the HP offspring, next, we evaluated whether this effect was due to direct changes in cellular functions or are indirect through a paracrine mechanism. For osteoblast, ex vivo primary mouse calvarial osteoblasts (MCOBs) were cultured from the newborn pups of C and HP fed dams (Fig. 4a). BrdU cell proliferation ELISA of pre-osteoblasts, ALP assay, and alizarin red staining of differentiated MCOBs showed a decrease in proliferation, differentiation, and mineralization, respectively, of HP group cells as compared to C (Fig. 4b–e). Besides, qPCR analysis for the mRNA levels of osteoblast marker genes *Runx2, Atf4, Col1a1, Osx*, and

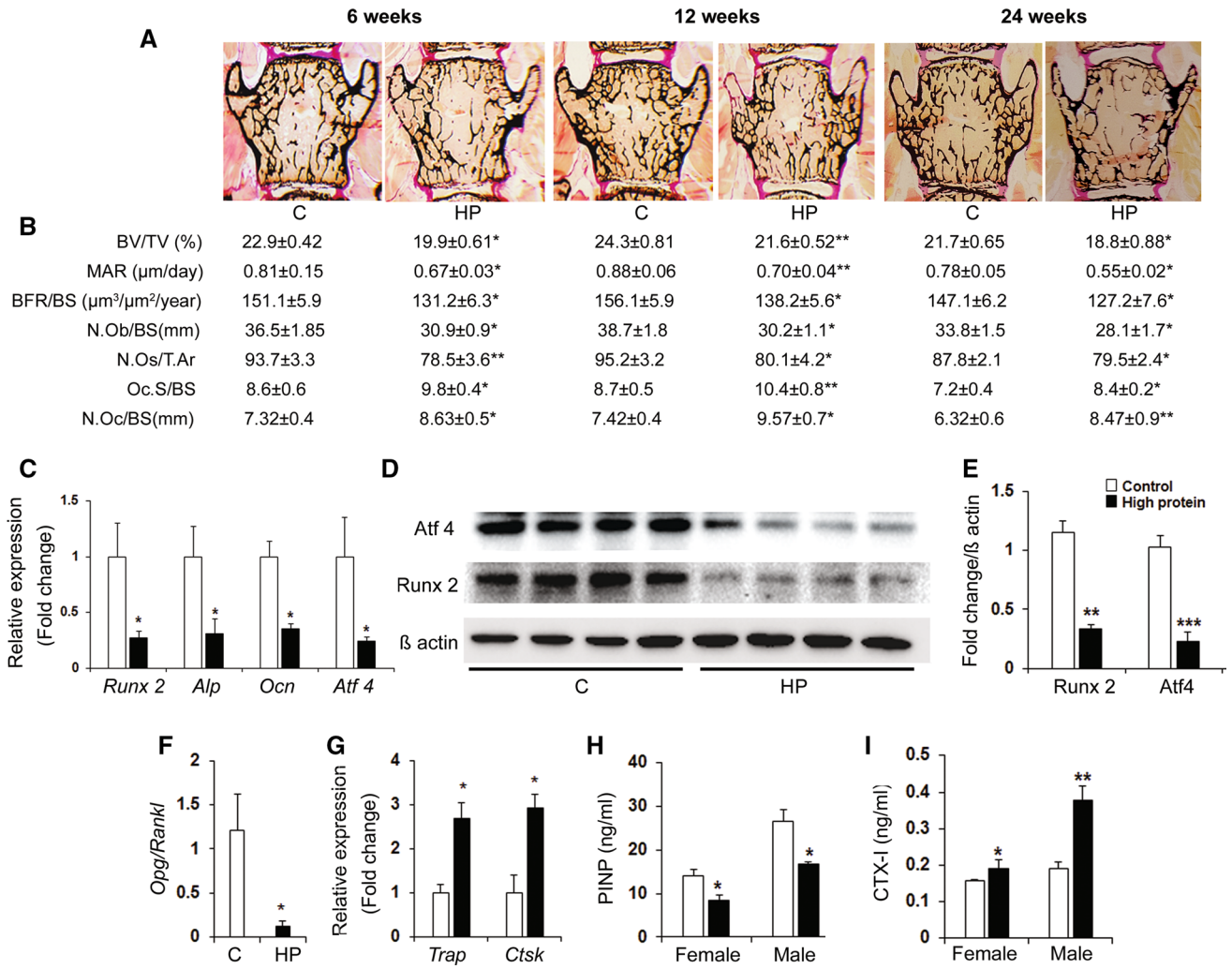

Fig. 3 Maternal HP induces decrease in bone formation and increase in bone resorption of the offspring: **a** Representative images of von kossa stained vertebral sections (Lumbar 4) of C and HP group female 6, 12 and 24-week-old offspring. **b** Measurements of bone volume/tissue volume (BV/TV), mineral apposition rate (MAR), bone formation rate per bone surface (BFR/BS), osteoblast numbers per bone surface (N.Ob/BS), osteocyte number per bone area (N.Os/T. Ar) osteoclast numbers per bone surface (N.Oc/BS) and osteoclast surface per bone surface (Oc.S/BS). **c** Real-time PCR analysis, **d** western blotting and **e** quantification of osteoblast marker genes from long bones of C and HP group female adult offspring. Real-time PCR analysis of **f** *Opg/Rankl* and **g** Osteoclast marker genes from long bones of C and HP group female adult offspring. Levels of bone turn over markers **h** P1NP in serum and **i** urinary CTX-1 levels in male and female adult offspring. Each group contains ≥ 6 animals. Data are presented as mean ± S.E.M. (*$P < 0.05$, **$P < 0.01$, ***$P < 0.001$)

Ocn were also found to be decreased in the HP group cells as compared to C (Fig. 4f). Interestingly, *Opg/Rankl* ratio was decreased in HP group MCOBs (Fig. 4g). Consistent with the qPCR results, western blot analysis of Runx2 and Atf4 also revealed a significant reduction in their protein expression levels from HP group MCOBs as compared to C (Fig. 4h–j).

Next, we evaluated the effect of maternal HP exposure on the offspring's osteoclastogenesis. For this purpose, we collected long bones from 12-week-old adult offspring and performed ex vivo BMCs osteoclast culture (Fig. 4k) from both HP and C groups. Results revealed no change in osteoclast cell differentiation (Fig. 4l–o) and osteoclast marker genes expression (Suppl. Figure 1) between C and HP groups in both male and female offspring.

These results suggested that there was a declined osteoblast cell activity without any change in osteoclast cell differentiation in the offspring from HP fed mothers.

Effect of maternal HPD on the miRNA expression and activity in the osteoblasts

To study the potential involvement of miRNAs in the maternal HPD modulated Ob cell activity, we performed small RNA sequencing and analyzed the differentially expressed miRNAs between ex vivo cultured MCOBs from

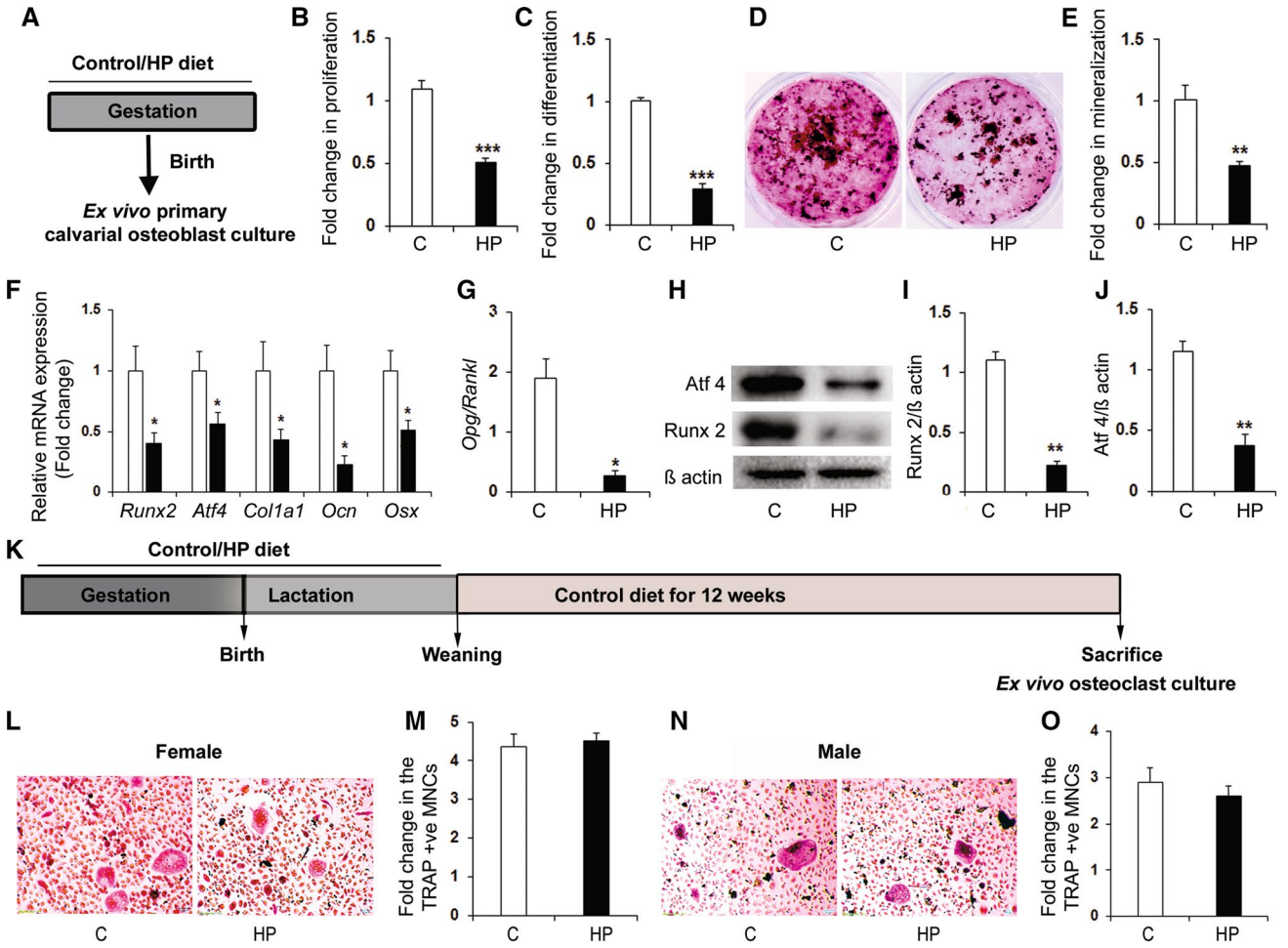

Fig. 4 Maternal HP negatively regulates osteoblast cell functions without any effect on osteoclast cell differentiation. **a** Schematic representation of experimental design for ex vivo MCOB culture. **b** BrdU incorporation assay, **c** Alkaline phosphatase activity, **d**, **e** Alizarin red staining, its quantification, **f** qPCR analysis of osteogenic genes, **g** *Opg/Rankl*, **h**, **j** western blotting and its quantification from the ex vivo cultured MCOBs of C and HP group offspring. **i** Schematic representation of experiment design for ex vivo BMC culture. **l**, **n** Representative images of TRAP stained osteoclast cells and **k**, **m** fold change in the number of TRAP+ multinucleated cells from the ex vivo BMC culture from C and HP group offspring. Each experiment was repeated three times, with a minimum of three replicates. Data are presented as mean ± S.E.M. (*$P < 0.05$, **$P < 0.01$, ***$P < 0.001$)

HP and C groups. Figure 5a shows the heat map of differentially expressed miRNAs. The results were confirmed by qPCR of 5 upregulated and 5 downregulated miRNAs (Suppl. Figure 2). Amongst the differentially expressed miRNAs, mmu-miR-24-1-5p was the most significantly and highest upregulated miRNA in the HP group. The increase in the expression was confirmed through TaqMan RT-qPCR in both MCOBs and adult offspring bone of HP offspring (Fig. 4b, c). RT-qPCR for the expression of miR-24-1-5p showed that while it was highly expressed in the bone tissue (Suppl. Figure 3), MCOBs cultured under osteogenic differentiation condition had a decrease in its expression with the number of days in culture (Fig. 5d). To further investigate the role of miR-24-1-5p on osteoblast cell function, we transfected miR-24-1-5p mimic and inhibitor with their respective negative controls in MCOBs. qPCR results showed an increase in its expression with mimic and a decrease in its expression with the inhibitor (Fig. 5e). The proliferation and differentiation of MCOBs were significantly decreased when transfected with miR-24-1-5p mimic, whereas inhibition of miR-24-1-5p markedly enhanced the same (Fig. 5f–g). Furthermore, matrix mineralization assessed by alizarin red staining and its extraction showed a reduction by the mimic and an increase by the inhibitor (Fig. 5h, i). qPCR for the mRNA expressions of *Runx-2, Atf-4, Col1a1, Ocn, and Osx* showed a downregulation by the mimic and upregulation by the inhibitor transfection in MCOBs. *Opg/Rankl* also followed the same profile with the mimic and inhibitor transfection (Fig. 5j).

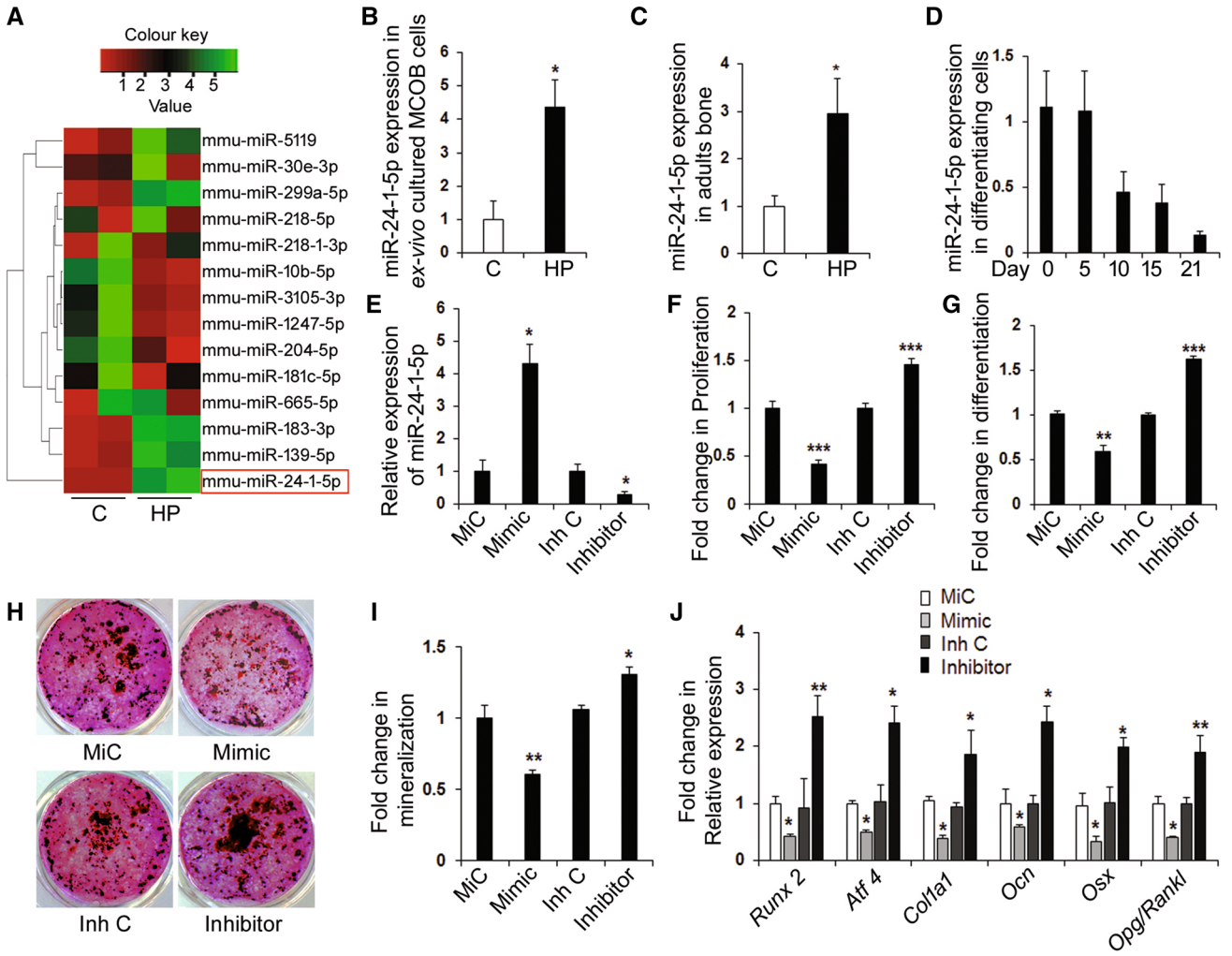

Fig. 5 Maternal HP upregulates osteoblastic expression of mmu-miR-24-1-5p, which inhibits osteoblast cells maturation. **a** Heat map showing differentially expressed miRNAs in the ex vivo cultured MCOBs of C and HP group offspring. Real-time PCR validation of miR-24-1-5p expression in **b** ex vivo cultured MCOBs and **c** the long bones of adult offspring, **d** Real-time PCR analysis of miR-24-1-5p expression in differentiating normal primary MCOBs. **e** Real-time PCR analysis of miR-24-1-5p expression in mimic and inhibitors transfected primary MCOBs. **f** BrdU incorporation assay, **g** alkaline phosphatase activity, **h**, **i** alizarin red staining and its quantification in mimic and inhibitors transfected primary MCOBs. **j** Real-time PCR analysis of osteoblast marker genes in miR-24-1-5p mimic and inhibitor transfected MCOBs. Each experiment was repeated three times, with a minimum of three replicates. Data are presented as mean ± S.E.M. (*$P < 0.05$, **$P < 0.01$, ***$P < 0.001$)

Evaluation of miR-24-1-5p target in the osteoblast cells

To further characterize the role of miR-24-1-5p in osteoblast function, we first predicted its putative target genes through bioinformatics tools (Target Scan, miRmap, miRDB, miRBase). We found that Smad-5, a key transcription factor downstream of BMP-2, contained a putative 7mer-m8 binding site of miR-24-1-5p in its 3′UTR between positions 2098–2104 (Fig. 6a). To check whether Smad-5 is a direct target of miR-24-1-5p, a dual-luciferase reporter assay was performed. The 3′UTR of *Smad-5* containing either wild type or mutant sequence in the predicted binding site was cloned into a p-miR-GLO plasmid (Fig. 6b) and co-transfected with either mimic or mimic control. Transfection of miR-24-1-5p mimic significantly downregulated luciferase activity in PGK-*Smad5*-3′UTR (wild type) transfected cells. In contrast, miR-24-1-5p transfection did not affect the luciferase activity of the mutated 3′UTR transfected cells (Fig. 6c). Next, to further validate these results, we performed western blotting for Smad-5 from the ex vivo cultured newborn's MCOBs (Fig. 6d) and bones of the adult (Fig. 6e), offspring from the maternal HP and C groups. We observed an expected reduced protein expression of Smad-5 in the HP group. Transfection of miR-24-1-5p mimic to MCOBs showed a decrease in Smad5 protein levels and a

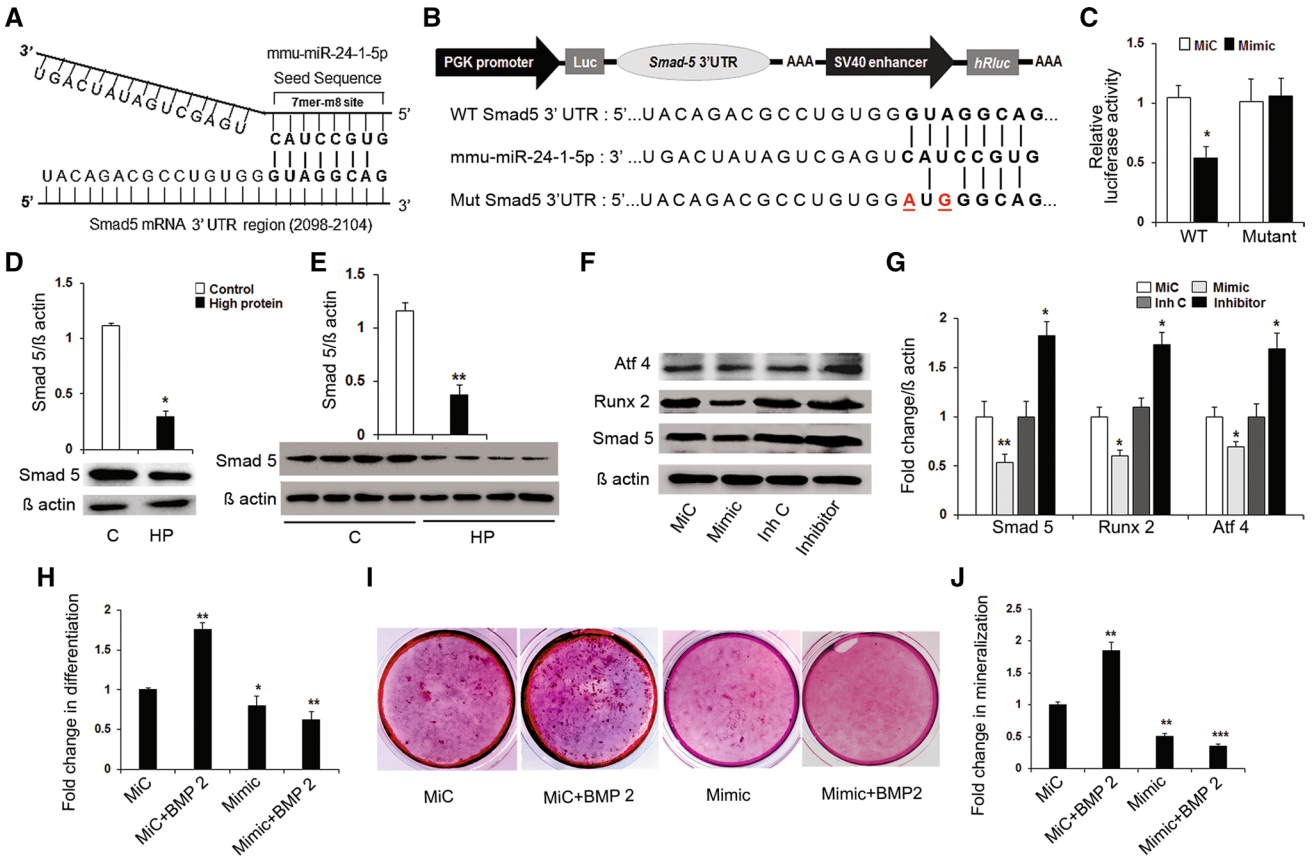

Fig. 6 miR-24-1-5p directly targets *Smad5* and blunts BMP2 activity. **a** Representation of miR-24-1-5p seed sequence that targets the Smad5 3′UTR region. **b** Schematic representation of cloning of Smad-5 3′UTR wild type (WT) or mutant (Mut) in the mammalian expression vector (pmirGLO). **c** Luciferase activity of WT Smad5 3′UTR or Smad5 3′ UTR mutant transfected MCOBs treated with miR-24-1-5p mimic or negative control (MiC). Western blot analysis of Smad5 in **d** the ex vivo cultured MCOBs and **e** long bones of adult offspring from C and HP group. **f** Western blot analysis of Smad5, Runx2, and Atf4 protein expression levels in miR-24-1-5p mimic and inhibitor transfected MCOBs and their **g** quantification. **i** Alkaline phosphatase activity, **j** Alizarin red staining, and **k** quantification in miR-24-1-5p mimic or MiC transfected MCOBs with or without BMP2 treatment. Each experiment was repeated three times, with a minimum of three replicates. Data are presented as mean ± S.E.M. (*$P < 0.05$, **$P < 0.01$, ***$P < 0.001$)

consequent downregulation of the expression of the osteogenic genes (Fig. 6f, g). In contrast, miR-24-1-5p inhibitor transfection markedly increased their expression (Fig. 6f, g).

Finally, we assessed how miR-24-1-5p mimic affects BMP2 action in the MCOBs as SMAD5, which is critical for BMP2 response is its target. To test that, we treated MCOBs transfected with or without miR-24-1-5p mimic with BMP2. The results showed that BMP2 enhanced both osteogenic differentiation and matrix mineralization in MiC transfected cells. However, in the mimic transfected cells, there was no effect of BMP2 treatment (Fig. 7h–j).

Effect of the inhibition of miR-24-1-5p in the ex vivo cultured MCOBs from HP offspring

Next, to test whether miR-24-1-5p inhibition could rescue the negative regulation of osteogenic differentiation caused by targeting *Smad5* in HP group osteoblasts, we transfected the miR-24-1-5p inhibitor in MCOBs derived from C and HP group's newborn offspring. Taqman qPCR revealed that there was a significant reduction in miR-24-1-5p expression in both C and HP group MCOBs when transfected with the inhibitor as compared to the inhibitor control (Fig. 7a). Moreover, the transfection of the inhibitor in the HP MCOBs was able to bring back the expression of mir-24-1-5p to the levels of C inhibitor control MCOBs (Fig. 7a). Consistently, we also observed that the inhibition of miR-24-1-5p recovered the inhibition of proliferation, differentiation, and matrix mineralization in HP group MCOBs to the levels of C group MCOBs (Fig. 7b–e). Next, to further evaluate whether the inhibitor transfection in the HP MCOBs can rescue the reduced protein expression of Smad5 and its downstream transcription factors Runx2 and Atf4, we performed western blot analysis with C and HP group MCOBs. The results revealed

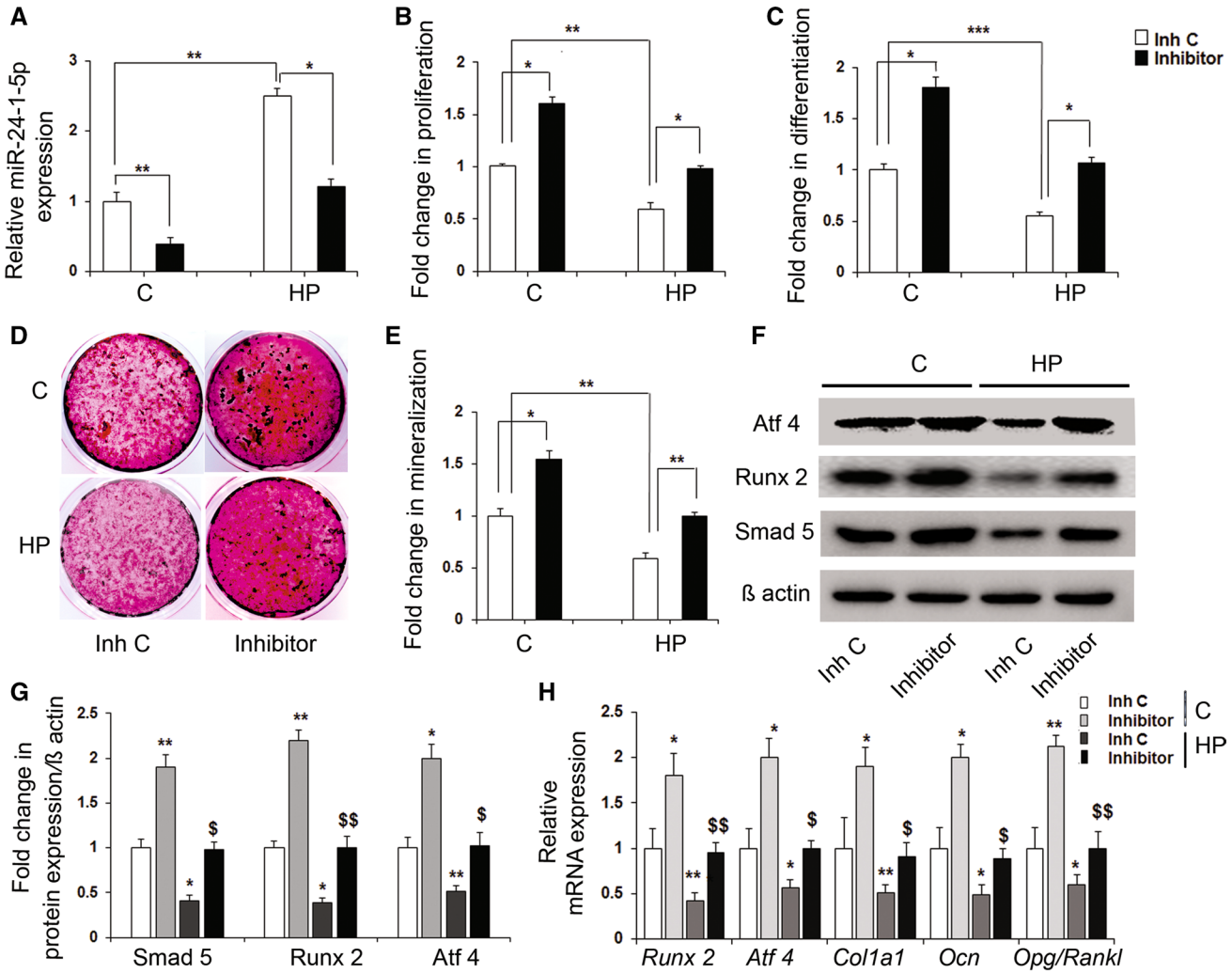

Fig. 7 Inhibition of miR-24-1-5p in the HP group offspring's ex vivo cultured MCOBs rescues the negative effect of maternal HP diet on osteoblast functions. **a** Real-time PCR analysis of miR-24-1-5p expression in miR-24-1-5p inhibitor transfected ex vivo cultured MCOBs of the C/HP group. **b** BrdU incorporation assay, **c** alkaline phosphatase activity, **d** alizarin red staining, and **e** its quantification in the miR-24-1-5p inhibitor transfected ex vivo cultured MCOBs of C/HP group. **f** Western blot analysis and **g** its quantification of in miR-24-1-5p inhibitor transfected ex vivo cultured MCOBs of C/HP group. **h** Real-time PCR analysis of osteoblast marker genes in miR-24-1-5p inhibitor transfected ex vivo cultured MCOBs of the C/HP group. Each experiment was repeated three times, with a minimum of three replicates. Data are presented as mean ± S.E.M. (*$P < 0.05$, **$P < 0.01$, ***$P < 0.001$)

that miR-24-1-5p inhibition significantly recovered the protein expression of these osteogenic markers (Fig. 7f, g). Furthermore, we evaluated the mRNA expression profile of the key osteogenic markers *Runx2, Atf-4, Col1a1, and Ocn* in the MCOBs transfected with the inhibitor by qPCR analysis. The expression profile of all these genes significantly recovered when miR-24-1-5p was inhibited in the HP group cells (Fig. 7h). Besides, the *Opg/Rankl* ratio also retrieved with the inhibitor treatment in the HP group MCOBs. Collectively these results suggest that miR-24-1-5p inhibition in osteoblast cell rescues the negative effect of maternal HP in MCOBs.

Discussion

Maternal nutrition plays an important role in optimizing the skeletal growth of the fetus and the offspring after birth [36]. An adequate supply of macronutrients and micronutrients during pregnancy is essential for the development of the growing fetus. Protein is one of the crucial macronutrients required for the growth of the fetal skeleton. While maternal low protein high carbohydrate diet has been shown to affect the offspring's bone mass negatively [17], some evidence suggests that the intake of a diet containing excessive protein and low carbohydrate during pregnancy may adversely affect fetal development [18, 37]. In the present study, we

further investigated the effect of maternal HP intake on the offspring's skeletal health in mice. Our results showed that the HP fed dams gained less weight as compared to the C dams during pregnancy and had a reduced litter size indicating a lower embryonic survival. In addition, the newborn offspring of HP dams had decreased weight and body length. These results were consistent with the animal and human studies, where similar results were found [37, 38]. During bone development, skeletogenesis occurs by two processes called intramembranous and endochondral ossification. While intramembranous ossification happens directly to make flat bones (craniofacial bones), endochondral ossification takes place by replacing a cartilage template to form the long bones [39]. Our evaluation of the newborn pup's skeleton showed a defective in utero growth and mineralization at both intramembranous and endochondral ossification sites in the HP group as compared to the C group. This effect was intelligible, as bone formation is an high energy demanding process and glucose is the preferred source of energy for the osteoblast cells [40]. However, with a HP diet the fetus must be dependent on the gluconeogenesis and hence the glucose availability must be lower resulting in a decreased mineralization. Next, we checked whether these changes in the newborn pup's skeleton persisted at later stages of life also even when they were weaned on a control diet, or there was a catchup growth. For that, the offspring from the C and HP groups were weaned on C diet and were analyzed for the changes in their bone microarchitecture by micro-CT at 6 weeks (growing age), 12 weeks (adult age), and 24 weeks (a later age). We selected these age groups of mice as they model different stages of bone homeostasis. At 6 weeks, bone modeling is prevalent, at 12 weeks, bone stays in equilibrium, and at 24 weeks, bone remodeling shifts more towards age-related bone loss. Our analysis of femur and tibia demonstrated that there was a loss of both trabecular and cortical bone structure in the HP group as compared to the C group pups at all the age groups. This effect was consistent in both male and female offspring. Together these results suggested that maternal HP leads to a permanent bone loss with no catchup growth and no sexual dimorphism. These results were consistent with some of the previous studies with different disease outcome, where the pathological condition was not rescued even when animals where shifted to normal diet [41–43]. One of the possible explanation could be that during in utero development the animal is programmed to deal with low glucose condition and is not able to utilize the normal glucose even when provided with it. Further research in this direction is required to delineate the role of carbohydrate and protein ratio during in utero development in the skeletal homeostasis at later stages.

To maintain a healthy structure, bone constantly undergoes remodeling, where a new mineralized matrix replaces the old matrix. This process takes place by the synchronized action of bone-forming osteoblast cells and bone-resorbing osteoclast cells [44]. We performed bone histology of lumber four vertebrae (LV4) from the female offspring to understand which arm of bone remodeling is affected in the HP group. Similar to the long bones, LV4 also showed a reduced bone mass in the HP group offspring at all the age groups. Besides, there was a decrease in bone formation due to a reduced osteoblast numbers and increased bone resorption because of increased osteoclast activity in the HP group. Decreased bone formation and increased bone resorption were also supported by the gene expression analysis of the femur and serum bone remodeling markers. Interestingly, *Opg/Rankl* ratio in the bones also decreased in the HP group. OPG and RANKL are the osteoclastogenic factors expressed by the osteoblast cells, and a reduced ratio means increased osteoclastogenesis [44, 45]. This observation indicated that the increased osteoclast number might be through the decreased *Opg/Rankl* ratio in the osteoblasts of HP group offspring. However, at this point, we were not clear whether the decrease in osteoblastogenesis and increase in osteoclastogenesis was due to cell autonomous, paracrine, or endocrine changes in the HP group offspring. Our ex vivo primary MCOB culture study from the C and HP group offspring showed that there was a decrease in the osteoblast cell proliferation, differentiation, and mineralization in the HP group cells, indicating a decreased osteoblast activity. This decrease was accompanied by a decline in the osteoblast marker genes transcription. Similar to the in vivo studies, protein levels of Runx2, a transcription factor essential for osteoblast early differentiation, and Atf4, which promotes matrix deposition [46], were also decreased in the HP group MCOBs. Consistently, *Opg/Rankl* ratio was also reduced in the HP group MCOBs. However, there was no change in the osteoclast differentiation between the ex vivo cultured BMCs from HP and C group offspring. These results demonstrated that while osteoblast cells from the HP group offspring were primed in utero to deposit less mineralized matrix, and increased osteoclastogenesis indirectly, there was no direct effect of maternal HP exposure on the offspring's osteoclast precursor cells.

Reports suggest that the changes in the epigenetic imprints during fetal development can hold the key to the development of future diseases [47, 48]. Interestingly, dietary factors can modify miRNA expression in the offspring and hence their later life health by targeting some critical genes expression [49–51]. However, their influence on bone mass regulation is mostly unidentified. Our small RNA sequencing studies revealed that miR-24-1-5p was most significantly and highest upregulated among various others miRNAs in HP group MCOBs, whose increased expression persisted even in the adult offspring's bone. In healthy adult mice, its expression was highest in the bones as compared to other tissues. Besides, miR-24-1-5p

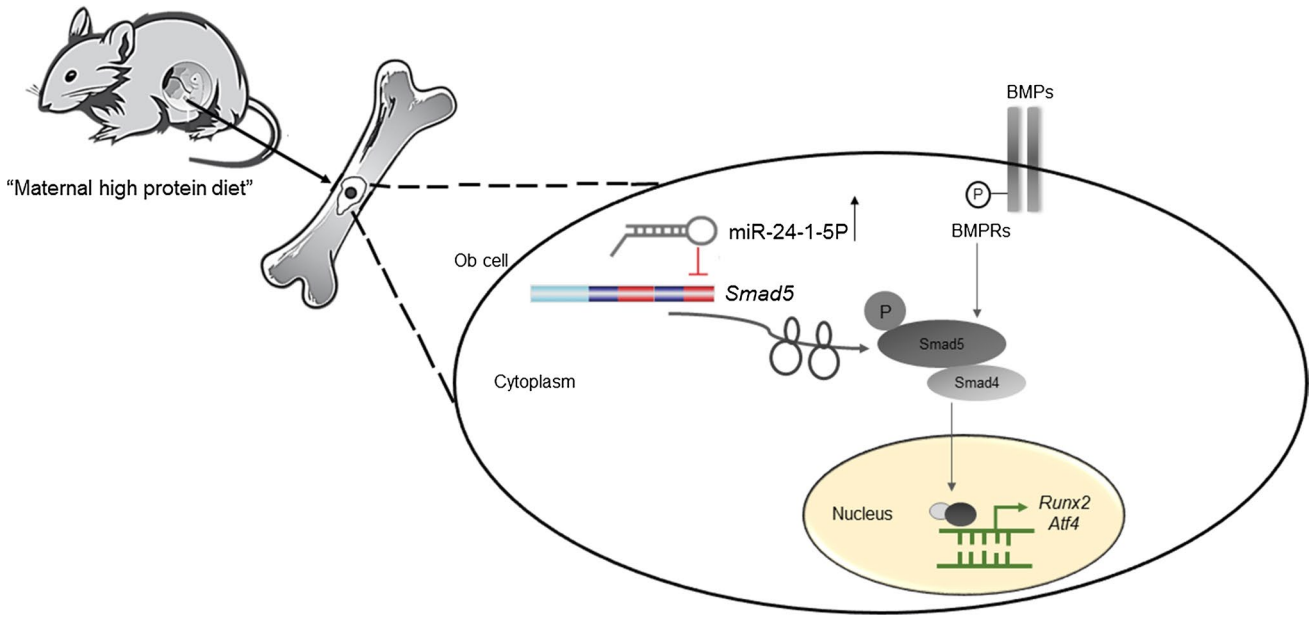

Fig. 8 Diagrammatic representation of the mechanism by which maternal HP diet regulates offspring's bone mass

expression decreased with increased osteoblast differentiation in normal MCOBs, indicating its suppressive influence in osteoblast cell maturation. Our investigation in the MCOBs revealed that miR-24-1-5p mimic transfection inhibits osteoblasts progression towards mineralizing phenotype, and inhibition of miR-24-1-5p promotes the same. To understand the relation of miR-24-1-5p with the osteoblast maturation and bone formation, we looked for possible targets of miR-24-1-5p. Our search revealed that the 3′ UTR of Smad5 has a 7mer-m8 perfect match site to the miR-24-1-5p seed region. Luciferase reporter experiment confirmed that miR-24-1-5p directly targets the Smad5 3′ UTR. Western blotting of Smad5 in the HP group offspring's MCOBs and adult bone also showed a decreased Smad5 expression as compared to the C group. Additionally, with mimic and inhibitors studies, we found an inverse association between expression levels of Smad5 and miR-24-1-5p. These results reestablished the relation between the two. SMAD5 is a critical downstream transcription factor for BMP2. Smad5 phosphorylation due to BMP2 signaling leads to a Smad5 complex formation, which translocates into the nuclei to transactivate the expression of osteogenic genes like *Runx2 and Atf4* [52–54]. Previous studies have confirmed its essential role in skeletal development and bone formation [55, 56]. In our results we found that HP group MCOBs had decreased Smad5 levels and hence decrease in its phosphorylation (data not shown). Besides, we found that miR-24-1-5p mimic transfection in the MCOBs blunts the BMP2 osteogenic effect. These results corroborate that miR-24-1-5p inhibits osteoblast maturation and matrix mineralization by targeting Smad5.

Next, we explored whether normalizing the elevated levels of miR-24-1-5p in the HP group offspring's ex vivo cultured MCOBs can rescue their cellular phenotype. Our results suggested that, indeed, transfection of miR-24-1-5p inhibitor in the HP group MCOBs can reverse the decrease in their proliferation differentiation and mineralization. Likewise, it also stabilized the decreased protein levels of Smad5 and its downstream genes, Runx2 and Atf4. A qPCR analysis also showed normalization of the osteogenic marker genes expression and, most notably *Opg/Rankl* ratio. These results further corroborated our previous findings, where we found that HP group offspring's osteoblasts overexpress miR-24-1-5p, which in turn impinge a negative effect on their skeleton through targeting Smad5 (Fig. 8).

In conclusion, the present study demonstrates that a maternal HP diet during pregnancy and lactation not only results in stunted and under-mineralized offspring's skeleton at birth but also the pups get primed for reduced bone mass throughout their life. These effects were due to an aberrant osteoblast cells function in the HP group offspring. Molecular investigations revealed that HP group osteoblasts overexpress miR-24-1-5p, which targets Smad5, an essential protein for osteoblast maturation. Moreover, inhibition miR-24-1-5p in the HP offspring's ex vivo cultured osteoblasts restore their normal cellular phenotype.

Acknowledgements We thank Dr. Naibedya Chattopadhyay (CSIR-Central Drug Research Institute, Lucknow, India) for the μ-CT facility

and Genotypic Technology Private Ltd. (Bangalore, India) for the small RNA sequencing and analysis.

Funding information This study was supported by Department of Biotechnology, Government of India. Funding from the Science and Engineering Research Board (SERB), Government of India (KS), and research fellowship grants from the Department of Science and Technology (GE) are also acknowledged.

Compliance with ethical standards

Conflict of interest The authors declare no conflict of interest in regard to this manuscript.

References

1. Cooper C et al (1997) Growth in infancy and bone mass in later life. Ann Rheum Dis 56(1):17–21
2. Cooper C et al (2002) The fetal origins of osteoporotic fracture. Calcif Tissue Int 70(5):391–394
3. Jordan KM, Cooper C (2002) Epidemiology of osteoporosis. Best Pract Res Clin Rheumatol 16(5):795–806
4. Thompson JN (2007) Fetal nutrition and adult hypertension, diabetes, obesity, and coronary artery disease. Neonatal Netw 26(4):235–240
5. Cleal JK et al (2007) Mismatched pre- and postnatal nutrition leads to cardiovascular dysfunction and altered renal function in adulthood. Proc Natl Acad Sci USA 104(22):9529–9533
6. Stocker CJ, Arch JR, Cawthorne MA (2005) Fetal origins of insulin resistance and obesity. Proc Nutr Soc 64(2):143–151
7. Simmons R (2011) Epigenetics and maternal nutrition: nature v. nurture. Proc Nutr Soc 70(1):73–81
8. Goyal D, Limesand SW, Goyal R (2019) Epigenetic responses and the developmental origins of health and disease. J Endocrinol 242(1):T105–T119
9. Baird J et al (2011) Does birthweight predict bone mass in adulthood? A systematic review and meta-analysis. Osteoporos Int 22(5):1323–1334
10. Flanagan DE et al (1999) Reduced foetal growth and growth hormone secretion in adult life. Clin Endocrinol 50(6):735–740
11. Javaid MK et al (2006) Maternal vitamin D status during pregnancy and childhood bone mass at age 9 years: a longitudinal study. Lancet 367(9504):36–43
12. Zhu K et al (2014) Maternal vitamin D status during pregnancy and bone mass in offspring at 20 years of age: a prospective cohort study. J Bone Miner Res 29(5):1088–1095
13. Ganpule A et al (2006) Bone mass in Indian children-relationships to maternal nutritional status and diet during pregnancy: the Pune Maternal Nutrition Study. J Clin Endocrinol Metab 91(8):2994–3001
14. Villa CR et al (2016) Maternal vitamin D beneficially programs metabolic, gut and bone health of mouse male offspring in an obesogenic environment. Int J Obes 40(12):1875–1883
15. Suntornsaratoon P, Krishnamra N, Charoenphandhu N (2015) Positive long-term outcomes from presuckling calcium supplementation in lactating rats and the offspring. Am J Physiol Endocrinol Metab 308(11):E1010–E1022
16. Hastings-Roberts MM, Zeman FJ (1977) Effects of protein deficiency, pair-feeding, or diet supplementation on maternal, fetal and placental growth in rats. J Nutr 107(6):973–982
17. Mehta G et al (2002) Intrauterine exposure to a maternal low protein diet reduces adult bone mass and alters growth plate morphology in rats. Calcif Tissue Int 71(6):493–498
18. Andreasyan K et al (2007) Higher maternal dietary protein intake in late pregnancy is associated with a lower infant ponderal index at birth. Eur J Clin Nutr 61(4):498–508
19. Blumfield ML et al (2012) Systematic review and meta-analysis of energy and macronutrient intakes during pregnancy in developed countries. Nutr Rev 70(6):322–336
20. Rush D, Stein Z, Susser M (1980) A randomized controlled trial of prenatal nutritional supplementation in New York City. Pediatrics 65(4):683–697
21. Ota E et al (2012) Antenatal dietary advice and supplementation to increase energy and protein intake. Cochrane Database Syst Rev 9:CD000032
22. Sloan NL et al (2001) The effect of prenatal dietary protein intake on birth weight. Nutr Res 21(1–2):129–139
23. Rigueur D, Lyons KM (2014) Whole-mount skeletal staining. Methods Mol Biol 1130:113–121
24. Ali SJ et al (2019) Bone loss in MPTP mouse model of Parkinson's disease is triggered by decreased osteoblastogenesis and increased osteoclastogenesis. Toxicol Appl Pharmacol 363:154–163
25. Sharan K et al (2017) Regulation of bone mass through pineal-derived melatonin-MT2 receptor pathway. J Pineal Res 63(2):e12423
26. Ali SJ et al (2019) Chlorpyrifos exposure induces parkinsonian symptoms and associated bone loss in adult swiss albino mice. Neurotox Res 36(4):700–711
27. Roman-Garcia P et al (2014) Vitamin B(1)(2)-dependent taurine synthesis regulates growth and bone mass. J Clin Invest 124(7):2988–3002
28. Lewis KE et al (2017) Skeletal site-specific changes in bone mass in a genetic mouse model for human 15q11-13 duplication seen in Autism. Sci Rep 7(1):9902
29. Sharan K et al (2011) A novel quercetin analogue from a medicinal plant promotes peak bone mass achievement and bone healing after injury and exerts an anabolic effect on osteoporotic bone: the role of aryl hydrocarbon receptor as a mediator of osteogenic action. J Bone Miner Res 26(9):2096–2111
30. Bachagol D et al (2018) Stimulation of liver IGF-1 expression promotes peak bone mass achievement in growing rats: a study with pomegranate seed oil. J Nutr Biochem 52:18–26
31. Pahwa H, Khan MT, Sharan K (2020) Hyperglycemia impairs osteoblast cell migration and chemotaxis due to a decrease in mitochondrial biogenesis. Mol Cell Biochem 469:109–118
32. Gavva C et al (2020) Glycosaminoglycans from fresh water fish processing discard—isolation, structural characterization, and osteogenic activity. Int J Biol Macromol 145:558–567
33. Khan K et al (2012) [6]-Gingerol induces bone loss in ovary intact adult mice and augments osteoclast function via the transient receptor potential vanilloid 1 channel. Mol Nutr Food Res 56(12):1860–1873
34. Kureel J et al (2014) miR-542-3p suppresses osteoblast cell proliferation and differentiation, targets BMP-7 signaling and inhibits bone formation. Cell Death Dis 5:e1050
35. Kushwaha P et al (2016) MicroRNA 874-3p exerts skeletal anabolic effects epigenetically during weaning by suppressing Hdac1 expression. J Biol Chem 291(8):3959–3966
36. Hyde NK et al (2017) Maternal nutrition during pregnancy: intake of nutrients important for bone health. Matern Child Health J 21(4):845–851
37. Switkowski KM et al (2016) Maternal protein intake during pregnancy and linear growth in the offspring. Am J Clin Nutr 104(4):1128–1136
38. Walther T et al (2011) High-protein diet in lactation leads to a sudden infant death-like syndrome in mice. PLoS ONE 6(3):e17443
39. Dirckx N, Van Hul M, Maes C (2013) Osteoblast recruitment to sites of bone formation in skeletal development, homeostasis, and regeneration. Birth Defects Res C Embryo Today 99(3):170–191

40. Karner CM, Long F (2018) Glucose metabolism in bone. Bone 115:2–7
41. Maredsous C et al (2016) High-protein exposure during gestation or lactation or after weaning has a period-specific signature on rat pup weight, adiposity, food intake, and glucose homeostasis up to 6 weeks of age. J Nutr 146(1):21–29
42. Carlin G et al (2020) Perinatal exposure of rats to a maternal diet with varying protein quantity and quality affects the risk of overweight in female adult offspring. J Nutr Biochem 79:108333
43. Carlin G et al (2019) Maternal high-protein diet during pregnancy modifies rat offspring body weight and insulin signalling but not macronutrient preference in adulthood. Nutrients 11(1):96
44. Kenkre JS, Bassett J (2018) The bone remodelling cycle. Ann Clin Biochem 55(3):308–327
45. Tanaka S (2007) Signaling axis in osteoclast biology and therapeutic targeting in the RANKL/RANK/OPG system. Am J Nephrol 27(5):466–478
46. Jensen ED, Gopalakrishnan R, Westendorf JJ (2010) Regulation of gene expression in osteoblasts. BioFactors 36(1):25–32
47. Deodati A, Inzaghi E, Cianfarani S (2019) Epigenetics and in utero acquired predisposition to metabolic disease. Front Genet 10:1270
48. Gicquel C, El-Osta A, Le Bouc Y (2008) Epigenetic regulation and fetal programming. Best Pract Res Clin Endocrinol Metab 22(1):1–16
49. Dumortier O et al (2014) Maternal protein restriction leads to pancreatic failure in offspring: role of misexpressed microRNA-375. Diabetes 63(10):3416–3427
50. Alejandro EU et al (2014) Maternal diet-induced microRNAs and mTOR underlie beta cell dysfunction in offspring. J Clin Invest 124(10):4395–4410
51. Zhang J et al (2009) Maternal high fat diet during pregnancy and lactation alters hepatic expression of insulin like growth factor-2 and key microRNAs in the adult offspring. BMC Genomics 10:478
52. Wang RN et al (2014) Bone morphogenetic protein (BMP) signaling in development and human diseases. Genes Dis 1(1):87–105
53. Lee KS et al (2000) Runx2 is a common target of transforming growth factor beta1 and bone morphogenetic protein 2, and cooperation between Runx2 and Smad5 induces osteoblast-specific gene expression in the pluripotent mesenchymal precursor cell line C2C12. Mol Cell Biol 20(23):8783–8792
54. Karner CM, Lee SY, Long F (2017) Bmp induces osteoblast differentiation through both Smad4 and mTORC1 signaling. Mol Cell Biol 37(4):e00253-16
55. Nishimura R et al (1998) Smad5 and DPC4 are key molecules in mediating BMP-2-induced osteoblastic differentiation of the pluripotent mesenchymal precursor cell line C2C12. J Biol Chem 273(4):1872–1879
56. Yamamoto N et al (1997) Smad1 and smad5 act downstream of intracellular signalings of BMP-2 that inhibits myogenic differentiation and induces osteoblast differentiation in C2C12 myoblasts. Biochem Biophys Res Commun 238(2):574–580